Numerical Studies of the Thermal Flowfield in a High-Temperature Non-Uniform Sphere Packed Bed

Uzu-Kuei Hsu¹, Chang-Hsien Tai^{2*}, Shih-Peng Lin²

¹Department of Aircraft Engineering, Air Force Institute of Technology

²Department of Vehicles Engineering, National Pingtung University of Science and Technology

ABSTRACT

When the sinter drops into the sinter cooler, the segregation causes the larger sizes to usually accumulate closer to the inner wall, and the smaller sizes to accumulate toward the outer wall. This situation causes non-uniformity in the overall sinter cooling due to the difference in the forced convection airflow between the outer and inner walls. This study uses the CFD (Computational Fluid Dynamics) approach with a porous media model, and directly simulation for a sphere packed bed, to understand the three types of inflow and heat transfer phenomena of high-temperature sinters in space. Also, the results may verify the reliability of the numerical simulating porous media model. It was found that the porous media model was unable to obtain the detailed temperature distribution inside the sinter, and might cause an error with the actual situation. The reason was that this method used a macro-perspective view to discuss the overall flow field of the sinter and effective heat transfer, and as a result was unable to obtain the detailed internal temperature distribution within the sinter. Therefore, in order to understand the heat transfer phenomena of the sinter packed bed, the establishment of an external geometric structure is still required.

Keywords: Sinter, Sphere packed bed, Porous media, CFD.

高温非均匀球槽床熱流場之數值研究

徐子圭¹、戴昌賢^{2*}、林世逢²
¹空軍航空技術學院飛機工程系
²國立屏東科技大學車輛工程學系

摘要

燒結礦在製成後落至冷卻機時,因落料偏析導致燒結礦內側粒徑較大外側較小,此情況將導致內外側燒結礦因受強制對流大小的差異,使得整體冷卻機散熱不均勻,燒結礦出口處溫差過大,而造成輸送帶的變形。本研究藉由數值模擬二維多孔介質模式與球型堆疊床方式,了解高溫燒結礦在空間中三種排列方式的流場與熱傳現象,並相互驗證數值模擬多孔介質模式的真實性,其中發現以多孔介質方式所模擬之溫度場結果並無法滿足實際情形,因為此方式以巨觀角度探討整體燒結礦之流場與等效熱傳,以致於無法詳細得知燒結礦內部溫度分佈,因此,若要了解燒結礦堆疊床的熱傳現象,仍須以建立幾何外型的方式進行。

關鍵字:燒結礦、球型堆疊床、多孔介質、計算流力。

^{*}通訊作者/ Corresponding author: e-mail:chtai@mail.npust.edu.tw

1. Introduction

Sinter is one of the main raw materials for producing molten iron within blast furnaces. However, due to the various particle sizes after the production (0.05m-0.2m), and as the temperature reaches as high as 900 K, the sintered particles must first pass through the sinter cooler before entering the silo to protect the conveyor from burn damage. When the sinter drops into the sinter cooler, the segregation causes the larger sizes to usually accumulate closer to the inner wall, and the smaller sizes to accumulate toward the outer wall. This situation causes non-uniformity in the overall sinter cooling due to the difference in the forced convection airflow between the outer and inner walls. When serious, the overlarge temperature difference at the exit causes deformation of the conveyor. The sinter within the passages of the sinter cooler could be seen as a porous medium where fluid is able to flow through, where the geometric shapes of the particles themselves appear to be irregular. Therefore in this study, the sinter pressure drop and heat transfer characteristics obtained by experimental data [1] were substituted into the numerical simulation porous media model in order to understand the flow field and heat transfer phenomena. Also, the results may verify the reliability of the numerical simulating porous media model. It was found that the numerical simulation results had verified that the temperature field of the porous media approach was unable to meet with the actual situation. The reason was that although larger sinter particles received a larger forced convection and allowed the temperature surface to drop more rapidly, the large particles were unable to effectively dissipate the heat inside. This temperature

accompanies the sinter as these large particles drop onto the conveyor, and cause burn damages to the conveyor as these particles break up. Darcy [2] studied the resistance characteristics of the porous media vessel at low Reynolds numbers, and discovered that the pressure difference caused by flowing fluid was proportional to the flow rate, and further defined the permeability (K) for the porous medium. When the permeability (K) was greater, the fluid was able to flow more easily within the porous medium. However, this theory only applies when the Reynolds number is greater than 1. Forchheimer [3] had indicated when the speed of the fluid was instead larger, the form drag generated by the solids of the porous media, and the surface drag caused by friction, would seriously affect pressure drop. Brinkman [4] had proposed that the friction of the wall must be considered for a limited space, and when the wall is impenetrable in order to meet with the non-slip condition of the wall. Andrade et al. [5] studied the classical Darcy's law by numerical simulation of a two-dimensional porous media where the pore size distribution is irregular. The Forchheimer equation was used to modify the correlation equation of different porosities and flow fields, and had found through experiments that when the Reynolds number higher, the inertial effect would accordingly increase, and would transform from a linear to a non-linear relationship. Amiriet et al. [6] used numerical simulation to study the forced convection in sphere packed beds. The liquid and solid energy equations, heat dissipation effect, changes with the porosity, the inertia effect and solid boundary effect were considered, respectively. If any of the above assumptions was not taken into consideration, the study results would cause

error. Sozen et al.[7] analyzed the vapor condensation phenomenon while transient forced convection was applied to the sphere packed bed. Caliset et al. [8] used numerical methods to explore the created pressure drop of the fluid within a three-dimensional packed bed, with experimental comparison. Tavman [9] analyzed the porous media, formed by the packed particles, and compared the difference between the various equivalent thermal conductivity coefficients with experimental results; which then indicated that a single equivalent thermal conductivity coefficient model is unable to apply to all cases, because the effective thermal conductivity of each solid to fluid ratio, and the porosity, of the porous media would affect the calculation for the equivalent thermal conductivity coefficient. Vafai et al. [10] considered the boundary and inertia effects of the solid, and used a local average volume approach to derive the transport equations for the flow and heat transfer in porous media. It was found that the solid boundary effects and non-Darcy effects had a significant effect to a flow field with a higher porosity, Prandtl number, and pressure gradient. Benenati et al [11] discovered the variable changing of the porosity of the inner walls. Chou et al. [12] studied how the channeling effect, caused by changes in porosity, influenced the flow field and temperature distribution within the porous media channels.

From the above literature review, it could be seen that many people had provided relevant empirical equations, from a macro view of the porous media, for sphere and irregular shaped packed beds, where experiments and numerical simulations had verified with each other to prove that the equations were considerably reliable [1]. In

contrast, the heat transfer analysis with the porous media rarely has complete numerical analysis results, though scholars experimental methods to propose related perspectives. However, as numerical simulation has been widely utilized in engineering, it is believed that the results may benefit future applications if a rather complete numerical simulation approach is established for the porous media flow field and temperature field. Nevertheless, from the numerical simulations in this study with a porous media model, and by comparing to the established two-dimensional sphere packed bed, it was found that the porous media model cannot fully show the internal temperature distribution inside the sinter particles, and resulted in an inability to determine whether the sinter is being cooled. Therefore, in order to understand the heat transfer phenomena of the sinter packed bed, the establishment of an external geometric structure is still required.

1. 2. Method of Research

2.1 Governing Equation

2.1.1 Continuity Equation

$$\frac{\partial \rho}{\partial t} + \nabla \cdot (\rho V) = 0 \tag{1}$$

2.1.2 Momentum Equation

(1) Porous Media Model:

$$\rho \left[(\vec{V} \cdot \nabla) \vec{V} + \frac{\partial \vec{V}}{\partial t} \right] = -\nabla p + \mu \nabla^2 \vec{v} + S_i$$
 (2)

(2) Sphere Packed Bed:

$$\rho \left[(\vec{V} \cdot \nabla) \vec{V} + \frac{\partial \vec{V}}{\partial t} \right] = -\nabla p + \mu \nabla^2 \vec{v}$$
 (3)

2.1.3 Energy Equations

(1) Porous media model:

$$\frac{\partial E}{\partial t} + \nabla \cdot (\vec{v}E + p\vec{u}) = k_{eff} \nabla^2 T + S_q \tag{4}$$

(2) Sphere packed bed:

$$\frac{\partial E}{\partial t} + \nabla \cdot (\vec{v}E) = k_{eff} \nabla^2 T \tag{5}$$

where S_i is the produced pressure loss as the fluid flow through the porous media, which follows the Brinkman- Forchheimer-Darcy equation, defined as below:

$$S_{i} = \frac{\partial p}{\partial x_{i}} = -\frac{\mu}{K} u_{i} - \frac{F\rho}{\sqrt{K}} u_{i}^{2}$$
 (6)

In the equation, E is the total energy, k_{eff} is the effective thermal conductivity, $S_q = \dot{m} (T_i - T_o)$, S_q is the heat transfer amount by the sinter, T_i is the temperature of the sinter when entering the cooler, T_o is the temperature of the sinter when exiting the cooler $\dot{m} = (1-\gamma)\rho_s C_s \vec{u} A$, \dot{m} is the released amount of heat, γ is the porosity, ρ_s is the sinter density, C_s is the sinter specific heat, and A is the cross section area.

2.2 Turbulence Model

In this study the standard $k-\varepsilon$ turbulent model, the most basic transport equation pair, is used to solve k and ε . The model is a turbulence model that is currently widely used in the industry, can be applied to a wide range of flow fields, and rather saves calculations; the coefficients in the equations are determined by water and air experiments toward the turbulence; the model does not consider the viscosity among the molecules. The transport equation s for the turbulence kinetic energy k and turbulent kinetic energy dissipation rate ε are:

$$\frac{\partial}{\partial x_i} \left(k \overline{u_i} \right) = \frac{1}{\rho} \frac{\partial}{\partial x_i} \left[\left(\mu + \frac{\mu_i}{\sigma_k} \right) \frac{\partial k}{\partial x_i} \right] + \frac{G_k}{\rho} - \varepsilon$$
 (7)

$$\frac{\partial}{\partial x_i} \left(\varepsilon \overline{u_i} \right) = \frac{1}{\rho} \frac{\partial}{\partial x_i} \left[\left(\mu + \frac{\mu_i}{\sigma_{\varepsilon}} \right) \frac{\partial \varepsilon}{\partial x_i} \right] + \frac{C_{I\varepsilon}}{\rho} \frac{\varepsilon}{k} \left(G_k \right) - C_{2\varepsilon} \frac{\varepsilon^2}{k}$$
 (8)

The terms in equation (6) and (7) are defined as follow:

$$G_k = \mu_t S_s^2 \tag{9}$$

$$S_s = \sqrt{2S_{ii}S_{ii}} \tag{10}$$

$$S_{ij} = \frac{1}{2} \left(\frac{\partial \overline{u_i}}{\partial x_j} + \frac{\partial \overline{u_j}}{\partial x_i} \right)$$
 (11)

where G is the term produced by turbulence kinetic energy, and $C_{1\varepsilon}=1.44$, $C_{2\varepsilon}=1.92$, $\sigma_{\kappa}=1.0$, $\sigma_{\varepsilon}=1.3$ and $C_{\mu}=0.09$ in the equations are empirical constants.

3. Physical Model and Boundary Conditions

3.1 Geometric Structure

3.1.1 Porous media model

The geometric structure of the numerical simulation porous media model is shown in Figure 1(a). The top is the sinter area at size 3×3 m^2 (H×L), and the bottom is the air inlet. Thus the overall size is 4×3 m^2 (H×L).

3.2 Exterior Shape of the Sphere Packed Bed

The sinter's exterior shape is complicated and irregular. To plot the exterior shape in detail is thus difficult and inefficient. The established sphere packed bed in this study is used to compare the simulation results with the porous media, and therefore used a sphere packed bed as the basic structure. The size of the sphere particles, which represented the sinter, was 0.05m-0.2m, and the overall sinter area was $3\times3~m^2~(\text{H}\times\text{L})$. The model was placed within a computational domain flow field, size $3\times4~m^2~(\text{H}\times\text{L})$, as shown in Figure 1(b).

3.3 Boundary Conditions

3.2.1 Boundary Conditions for the Porous Media Model

The fluid at the inlet was set as air, where the pressure was fixed at 2352 Pa, and temperature at 300 K. According to the actual situation of the sinter entering the cooler, the temperatures of the sinter particles themselves

would be different with the different particle sizes. The sinter temperature for the large particles was 900 K, and 500 K for the small ones. In addition, the temperature distribution was assumed to change linearly. The fluid outlet was simulated as the air flowing through the porous media and finally to the atmosphere, and therefore the exit boundary condition used the standard atmospheric pressure. Moreover, the fluid not only satisfied the impermeable condition: it was also made to obey the non-slip condition. As a result, the surrounding walls of the sinter cooler constituted an adiabatic non-slip wall. The sinter material determined through parameters were experiments [1], where the density was 3939 kgm⁻³, equivalent specific heat of the large sinter particles were 171.48 Jkg⁻¹K⁻¹, with an equivalent thermal conductivity coefficient of 3.82 $Wm^{-1}K^{-1}$; the equivalent specific heat of the small sinter particles were 168.76 Jkg⁻¹K⁻¹, with an equivalent thermal conductivity coefficient of 3.94 $Wm^{-1}K^{-1}$. Furthermore, according to literature, it is known that a single effective thermal conductivity model is unable to apply for every case. Therefore, to define the different sinter arrangements in this study, it was assumed that the porosity, viscous drag, inertial resistance, specific heat and effective thermal conductivity of the porous media changed linearly with the sinter size. Each parameter is listed in Table 1.

3.2.2 Boundary Conditions for the Sphere Packed Bed

The sphere packed bed was directly established by the sphere particles in the flow field, and therefore did not consider the sinter porosity, viscous resistance and inertial resistance during the calculating process. The sinter material parameters were the same as in Table 1, where the sinter temperature was set

at 900 K. The cooling air was fixed at a pressure of 2352 Pa and with an inlet temperature of 300 K, directly blowing towards the sinter. The fluid outlet was simulated as the air flowing through the porous media and finally to the atmosphere, and therefore the exit boundary condition used the standard atmospheric pressure.

Table 1 Sinter material parameters chart

Particle diameter, d_p (m)	0.001	0.05
Porosity,	0.395	0.545
Permeability, $K(m^2)$	9.1×10 ⁻⁹	5.20×10 ⁻⁸
Inertial coefficient, F	0.8043	0.225
Thermal conductivity $(Wm^{-1}K^{-1})$	3.94	3.82
specific heat, C_p $(Jkg^{-1}K^{-1})$	168.76	171.48

4. Results and Discussion

4.1 Flowfield of the Sinter Area

4.1.1 Porous media model

Three types of arranged patterns of the sinter particles on the cooler, due to the flow field by porosity changes, were discussed:

The arrangement method in Model A_1 is a horizontal distribution of large sinter particles and porosities on one end, and becoming smaller at the other end. Since the porosity is smaller for small sinter particles, the flow resistance was larger. From Figure 2(a), it could be seen that the vertical speed at the left side was smaller, and the fluid flowed toward the side which had larger porosities.

The arrangement method in Model A_2 is a horizontal distribution of large sinter particles and porosities located at the middle, and

becoming smaller toward both sides. Since the flow resistance at locations with large porosities was smaller, it could be seen from Figure 2(b) that the vertical speed at the middle was higher, where the fluid was flowing toward the middle.

The arrangement method in Model A_3 is a vertical distribution with large sinter particles

and porosities at the bottom and becoming smaller at the top. As a result, the air resistance at the air outlet at the top was large. From Figure 2(c), it could be seen as the air flows through the different sinter sizes, the overall vertical speed is small and even.

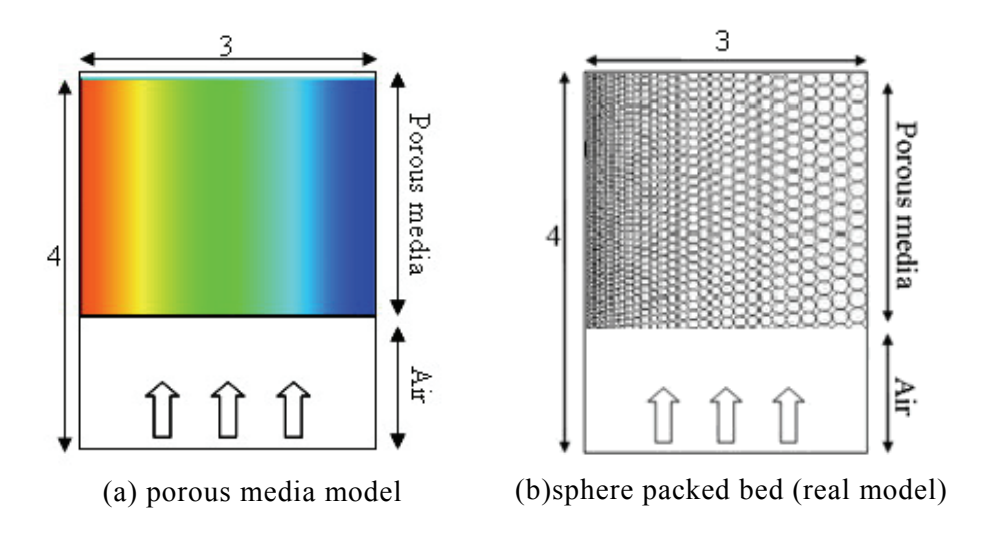


Figure 1. Numerical simulation of the geometric structure (unit: m)

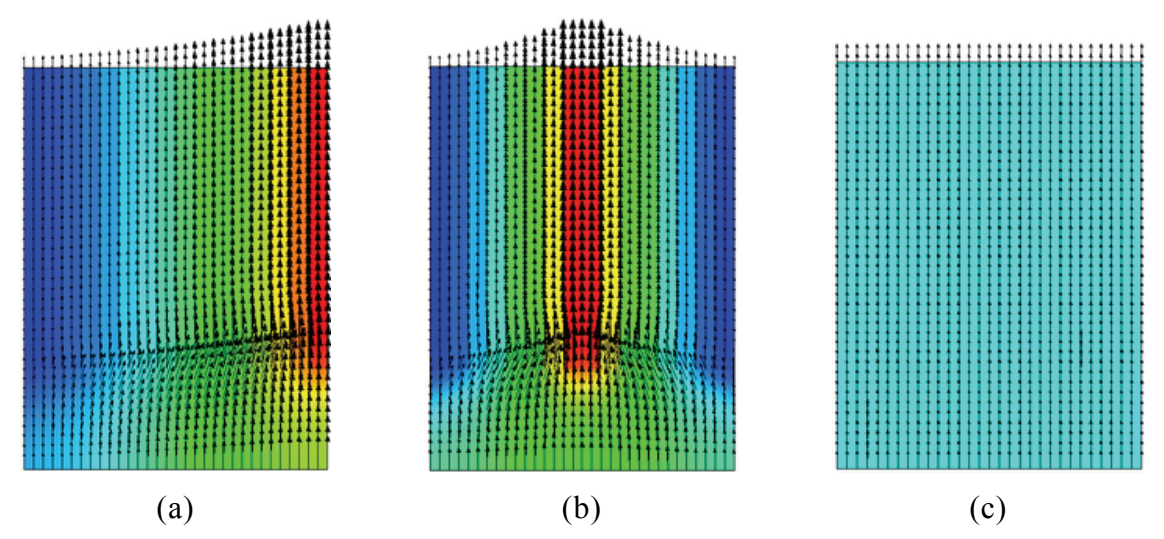


Figure 2. Vertical velocity profile for the porous media model

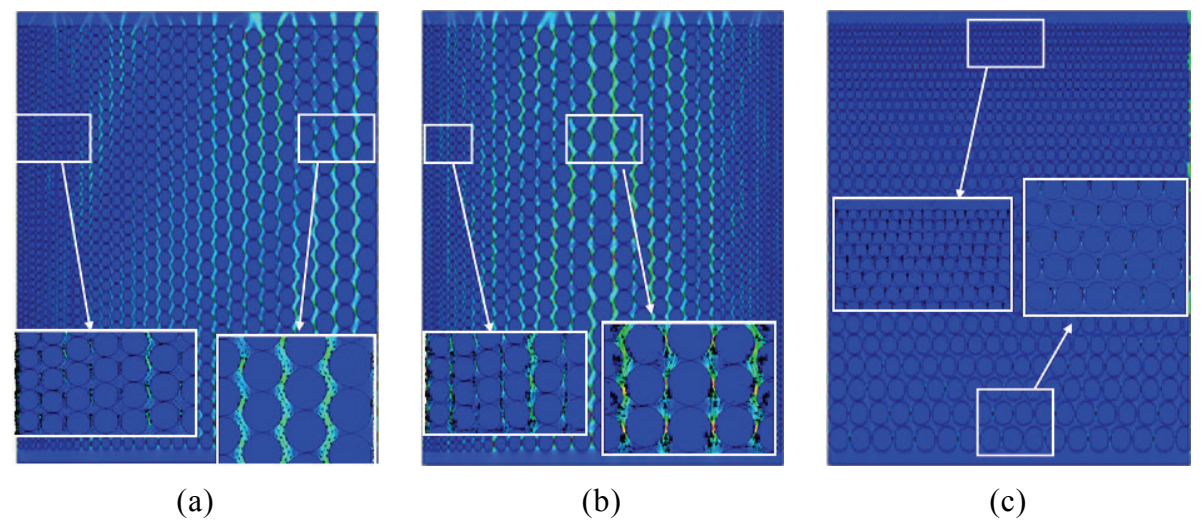


Figure 3. Vertical velocity profile for the sphere packed bed

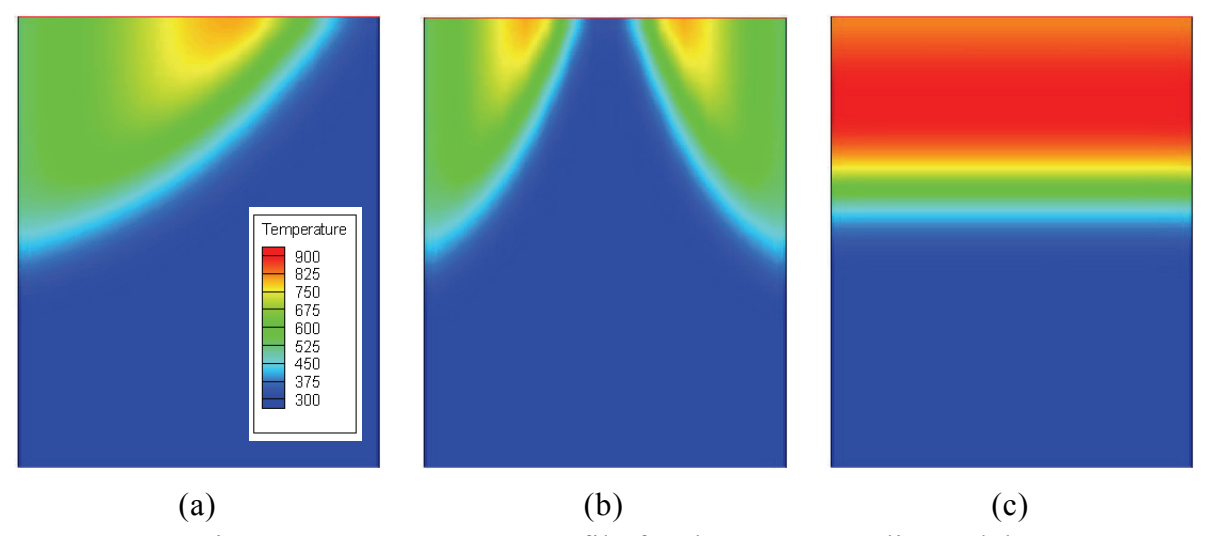


Figure 4. Temperature profile for the porous media model

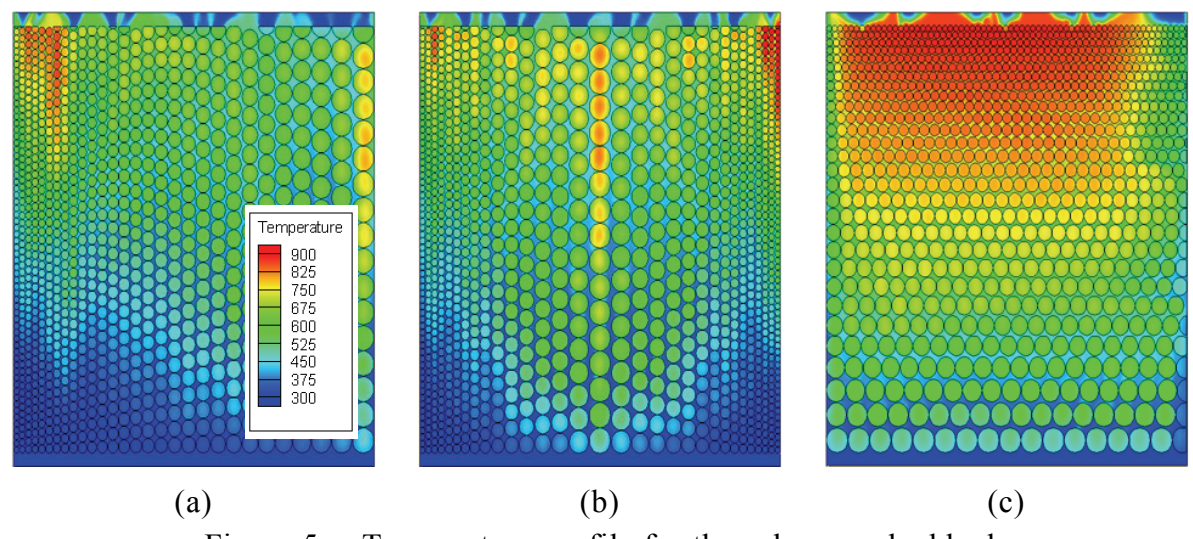


Figure 5. Temperature profile for the sphere packed bed

4.1.2 Sphere Packed Bed

As the sphere packed bed was directly established by the sphere particles in the flow field, the study was able to understand the flowing situations of the fluid from a more micro point of view. The discussions were as follows:

In Model A₁, the arrangement was a horizontal distribution of large sinter particles and porosities on one end, and becoming smaller at the other end. Since the inertial resistance of the air was smaller with larger particles, it was seen from Figure 3(a) that the average air velocity at the pores of the sinter particles was faster for large sinters than for small ones.

In Model A₂, the arrangement method was a horizontal distribution of large sinter particles and porosities located at the middle, and becoming smaller toward both sides. From Figure 3(b), it could be seen that as the inertial resistance for large porosities were smaller, therefore the average air velocity was larger at the middle and smaller at the two lateral sides.

In Model A₃, the arrangement method was a vertical distribution with large sinter particles and porosities at the bottom and becoming smaller at the top. From Figure 3(c), it was seen that the large inertial resistance at the top caused the cooling air to be unable to pass through the sinter. The overall sinter speed was rather smaller and even. As these results were compared with the numerical simulation results of the porous media, although the detailed situation of the fluid within the porous media model cannot be understood, the overall flow field trend was still similar with the sphere packed bed.

4.2 Temperature Field at the Sinter Area

4.2.1 Porous Media Model

The following discusses the numerical

simulation results of the sinter temperature field of the porous media. The arrangement methods of the sinter were previously in section 4.1:

The cooling situation in Model A_1 and Model A_2 are shown in Figures 4(a) & (b). Although the initial temperature of the large sinter particles was higher, these particles received a stronger enforced convection, thus the temperature was able to be cooled down faster than the smaller particle sizes. On the contrary, although the small sinter particles had the advantage of larger surface area of unit mass, the temperature was not easily cooled down due to smaller enforced convection.

The cooling situation in Model A₃ is shown in figure 4(c). Since the overall enforced convection is rather small, as the high temperatures carried by the large sinter particles are conducted (or by convection) to the small sinter particles, the heat accumulated at this location and was hard to dissipate.

4.2.2 Sphere Packed Bed

A sphere packed bed was used to explore the temperature distributions caused by different sinter arranging methods. The study was able to see more easily the heat convection of air and the thermal conductivity of the sinters. The summarization is as follow:

The temperature distribution in Model A_1 is shown in Figure 5(a). It can be seen that the temperature of the cooling air was higher when above small sinter particles, and the temperature was lower at large sinter particles. This reason was as described in Section 4.2.2, where when the air flows though small sinter particles, the larger inertial resistance causes the average flow speed to become smaller, and thus the heat was unable to quickly dissipate. The sinters at this location had yet shown no temperature drop. On the contrary, for the

large sinter particles, Figure 5(a) shows that although the surface temperature can quickly drop due to the larger enforced convection, the large particle itself causes the inside temperature to be unable to quickly spread to the surface, causing the formation of hot spots.

The temperature distribution in Model A_2 is shown in Figure 5(b). Although the arrangement method had changed, the temperature results were rather similar with Model A_1 . The heat concentrated above the small sinter particles and inside the large sinters.

The temperature distribution in Model A_3 is shown in Figure 5(c). From Section 4.2.2, it is known that the overall enforced convection is smaller, the high temperatures carried by the large sinter particles are conducted (or by convection) to the small sinter particles, the heat accumulated at this location and was hard to dissipate.

From the comparison with the two types of simulation methods, it could be seen that the porous media model used a macro view to explore the overall medium flow field and effective heat transfer characteristics. Therefore it was unable to show the complete temperature distribution inside the sinter particles. This may cause an error with the actual situation. From the comparison results, the overall heat dissipation by Model A₃ was the worst. However, for large sinter particles, this method may become more effective for dissipating heat.

5. Conclusions

By comparing the numerical simulation results of the sinter porous media model and the sphere packed bed for the flow field and temperature field, the following conclusions could be summarized:

- 1.Although the numerical simulation sinter porous media model was unable to explore the detailed flowing situation of the fluid within the medium, it was still very reliable for understanding the overall flow field.
- 2. This study discovered that the porous media model was unable to obtain the detailed temperature distribution inside the sinter, and might cause an error with the actual situation.
- 3. Therefore, in order to understand the temperature distribution of the medium in detail, the establishment of an exterior geometric structure is still required.
- 4.From comparison results, it can be seen that the overall cooling effect in Model A₃ was the worst. However, for large sinter particles, this method may become more effective for dissipating heat.

6. References

- 1.Uzu-Kuei Hsu, Chang-Hsien Tai, Kai-Wun Jin, 2009, "Investigation of the Thermo Flowfield in a Sinter Cooler with Different Array and Septum" Journal of Air Force Institute of Technology, Vol. 8, No. 1, pp. 253-262.
- 2.Darcy, H., 1856, Les fontains publiques de la ville de, Victor Dallmont, Paris.
- 3. Forchheimer, P., 1901, "Wasserbeweguing durch boden," *Z. Ver. Deutsch Ing.*, Vol. 45, pp. 1782-1788.
- 4. Kaviany, M., 1995, Principle of Heat Transfer in Porous Media Second Edition, Springer-Verlag New York.
- Andrada, J. S., Costa, Jr., U.M.S., Aleida, M. P., Makse, H. A., and Stanley, H. E., 1999, "Inertial effects on fluid flow through disordered porous media," *Physical Review Letters*, Vol. 82, pp. 5249-5252.
- 6.Amiri, A., and Vafai, K., 1994, "Analysis of

- dispersion effects and non-thermal equilibrium, non-Darcian, variable porosity incompressible flow through porous media," *Int. J. Heat Mass Transfer,* Vol. 37, pp. 939-954.
- 7.Sozen, M., and Vafai, K., 1990, "Analysis of non-thermal equilibrium condensing flow of a gas through a packed bed," *Int. J. Heat Mass Transfer*, Vol. 33, pp. 1247-1261.
- 8. Calis, H. P. A., Nijenhuis, J., Paikert, B. C., Dautzenberg, F. M., and Bleek, C. M., 2001, "CFD modeling and experimental validation of pressure drop and flow profile in a novel structured catalytic reactor packing," *Chemical Engineering Science*, Vol. 56, pp. 1713-1720.
- Tavman, I. H., 1996, "Effective thermal conductivity of granular porous materials," *Int. Comm. Heat Mass Transfer*, Vol. 24, pp. 169-176.
- 10. Vafai, K., and Tien, C. L., 1981, "Boundary and inertia effects on flow and heat transfer in porous media," *Int. J. Heat Mass Transfer*, Vol. 24, pp. 195-203.
- 11. Benenati, R. F., and Brosilow, C. B., 1962, "Void fraction distribution in a bed of spheres," *J. AICHE*, Vol. 8, pp. 359-361.
- 12.Chou, F. C., Lin, W. Y., and Lin, S. H., 1992, "Analysis and experiment of non-Darcian convection in horizontal square packed-sphere channel-part 1: forced convection," *Int. J. Heat Mass Transfer*, Vol. 35, pp. 195-206.